Controlled Synthesis and Water Dispersibility of Hexagonal Phase $NaGdF_4$:Ho^{3+}/Yb^{3+} Nanoparticles

Rafik Naccache, Fiorenzo Vetrone, Venkataramanan Mahalingam, Louis A. Cuccia, and John A. Capobianco*

Department of Chemistry and Biochemistry, Concordia University, Montreal H4B 1R6, Canada

Received November 19, 2008. Revised Manuscript Received December 22, 2008

The luminescence properties of hexagonal sodium gadolinium fluoride nanoparticles co-doped with Ho^{3+} and Yb^{3+} ($NaGdF_4$:Ho^{3+}/Yb^{3+}), prepared using a thermal decomposition synthesis route, were evaluated following 980 nm excitation. The synthesized nanoparticles were easily dispersed in nonpolar solvents, showed an extremely narrow particle distribution, and were determined to have a mean diameter of 15.6 ± 1.2 nm. The predominantly green upconversion emission was observed to increase with increasing Ho^{3+} concentration due to an enhanced energy transfer (ET) from the neighboring Yb^{3+} ions. Post-synthesis, the nanoparticles were dispersed in water via modification of the capping oleic acid (OA) ligand. Upconversion emission intensity was observed to decrease upon dispersion in aqueous media likely due to an increase in nonradiative decay pathways. A total ligand exchange with poly(acrylic acid) (PAA) resulted in slightly more intense upconversion emission relative to oxidation of the OA to azelaic acid.

Introduction

The search for highly emitting and efficient upconverting nanoparticles has been a pivotal driver for much of the current luminescence research.[1−5] Upconverting nanoparticles are extremely attractive for a multitude of applications, namely, in the field of bioimaging where researchers are evaluating novel approaches to in vivo imaging,[6,7] as well as disease detection and diagnostics.[8,9] Such applications require the nanoparticles to be in the form of a colloidal solution implying that the nanoparticles' surface (or the ligands coordinating the nanoparticles) should either be hydrophilic or at least amenable to functionalization allowing for a facile dispersion of the nanosolids in water or other biorelevant media. The advantage of aqueous-based colloidal solutions is the inherent compatibility with in vivo systems where the aqueous media do not impact the biological system and are not as highly cytotoxic.[10]

Consideration of cytotoxicity is not only limited to the medium used for in vivo administration but is also a principle concern for the luminescent component being dosed.[11] Preliminary studies seem to suggest that lanthanide-doped $NaYF_4$ nanoparticles have a low toxicity profile.[12a] For example, cell survival in MTT assays (3-(4,5-dimethylthiazol-2-yl)-2,5-diphenyltetrazolium bromide) was not affected when the cells where incubated with NaYF4 nanoparticles co-doped with Er^{3+} and Yb^{3+} nanoparticles solutions up to 0.5 mg/mL, which is significantly more elevated relative to the concentrations typically used for cell imaging. Consequentially, these lanthanide-doped nanoparticles may become a viable alternative to common dye-based techniques or even quantum dots (QDs).

The tripositive holmium ion (Ho^{3+}) is of great interest due to its strong green upconversion luminescence, which dominates the blue and red emission. Furthermore, Ho^{3+} possesses a very interesting spectral landscape. Much like the tripositive erbium (Er^{3+}) and thulium ions (Tm^{3+}), the bare spectral window ranging from 570−630 nm renders it ideal as a probe in fluorescence resonance energy transfer (FRET) and other biologically oriented applications.[9,13,14] Tripositive ytterbium (Yb^{3+}) is an ideal co-dopant ion since it possesses only one excited state, which can be easily excited using a wavelength of 980 nm typically available through inexpensive diodes. The absorption cross-section of the excited-state of the Yb^{3+} ion is significantly greater than many of the excited states of other lanthanides with similar energy levels rendering the upconversion/energy transfer

* To whom all correspondence should be addressed. E-mail: capo@vax2.concordia.ca.

(1) Boyer, J.-C.; Cuccia, L. A.; Capobianco, J. A. *Nano Lett.* **2007**, *7*, 847.
(2) Heer, S.; Kömpe, K.; Güdel, H.-U.; Haase, M. *Adv. Mater.* **2004**, *16*, 2102.
(3) Li, Z.; Zhang, Y. *Nanotechnology* **2008**, *19*, 345606/1.
(4) Mai, H.-X.; Zhang, Y.-W.; Sun, L.-D.; Yan, C.-H. *J. Phys. Chem. C* **2007**, *111*, 13721.
(5) Yi, G.-S.; Chow, G.-M. *Chem. Mater.* **2007**, *19*, 341.
(6) Chatterjee, D. K.; Rufaihah, A. J.; Zhang, Y. *Biomaterials* **2008**, *29*, 937.
(7) Lim, S. F.; Riehn, R.; Ryu, W. S.; Khanarian, N.; Tung, C.-K.; Tank, D.; Austin, R. H. *Nano Lett.* **2006**, *6*, 169.
(8) Nyk, M.; Kumar, R.; Ohulchanskyy, T. Y.; Bergey, E. J.; Prasad, P. N. *Nano Lett.* **2008**, *8*, 3834.
(9) Wang, L.; Yan, R.; Huo, Z.; Wang, L.; Zeng, J.; Bao, J.; Wang, X.; Peng, Q.; Li, Y. *Angew. Chem., Int. Ed.* **2005**, *44*, 6054.
(10) Abdul Jalil, R.; Zhang, Y. *Biomaterials* **2008**, *29*, 4122.
(11) Jamieson, T.; Bakhshi, R.; Petrova, D.; Pocock, R.; Imani, M.; Seifalian, A. M. *Biomaterials* **2007**, *28*, 4717.
(12) (a) Wang, F.; Chatterjee, D. K.; Li, Z.; Yong, Z.; Fan, X.; Wang, M. *Nanotechnology* **2006**, *17*, 5786. (b) Zhang, T.; Ge, J.; Hu, Y.; Yin, Y. *Nano Lett.* **2007**, *7*, 3203.
(13) Chen, Z.; Chen, H.; Hu, H.; Yu, M.; Li, F.; Zhang, Q.; Zhou, Z.; Yi, T.; Huang, C. *J. Am. Chem. Soc.* **2008**, *130*, 3023.
(14) Wang, F.; Liu, X. *J. Am. Chem. Soc.* **2008**, *130*, 5642.

10.1021/cm803151y CCC: $40.75
Published on Web 01/22/2009

processes much more efficient and has been well documented in the literature (see, for example, refs 15 and 16). Much of the current work in the literature has focused on the Er^{3+}/Yb^{3+} combination of ions in a myriad of hosts.[17−22]The Ho^{3+}/Yb^{3+} combination represents an attractive alternative to the Er^{3+}/Yb^{3+} counterpart as the green/red luminescence ratio of the latter can be greatly impacted by the lanthanide dopant concentration as well as the intrinsic phonon energy of the host.

The fluoride hosts such as the one studied in the current work are strong and efficient upconverters.[23−25] They possess several advantages relative to their counterparts (phosphates, oxides, etc.) in that they possess intrinsically low phonon energies and hence, the non-radiative bridging of the gaps separating the various energy level is compromised allowing for a strong and efficient upconversion.

The nanoparticles discussed in this work were prepared using a modified thermal decomposition method.[1,26,27] However, in the current work, the synthesis was carried out using a mechanical pump for the uniform and precise addition of the precursor solution to the ligand vessel, thereby eliminating any variation in the rate of addition, which can affect particle size, morphology, and luminescence intensity. A more thorough systematic study using the mechanical pump to investigate rates of addition and reaction time has been initiated and will be the subject of a future publication.

In this work, we report the upconversion luminescence properties of Ho^{3+}/Yb^{3+} co-doped sodium gadolinium fluoride ($NaGdF_4$:Ho^{3+}/Yb^{3+}) colloidal nanoparticles prepared using a thermal decomposition route. Since the synthesis yields nanoparticles capped with oleic acid, which can only be dispersed in nonpolar solvents (e.g., toluene, cyclohexane), we evaluate methods for rendering these nanoparticles dispersible in water. Luminescent properties of the nanoparticles were also evaluated following post-synthesis treatments.

Experimental Section

Thermal Decomposition Synthesis of Ho^{3+}/Yb^{3+} Co-Doped $NaGdF_4$ Nanocrystals. Gadolinium oxide (Gd_2O_3, 99.99+%), holmium oxide (Ho_2O_3, 99.999%), ytterbium oxide (Yb_2O_3, 99.99%), triflouroacetic acid (CF_3COOH, 99%), sodium trifluoroacetate (CF_3COONa, 98%), oleic acid (technical grade, 90%), and 1-octadecene (technical grade, 90%) were all purchased from Sigma-Aldrich and were used without further purification. The thermal decomposition synthesis described below is comprised of a two-step process where the first step involves the preparation of the trifluoroacetate lanthanide precursors, followed by the decomposition of the precursors, at elevated temperatures, and the formation of ligand-coordinated nanoparticles in the second step.

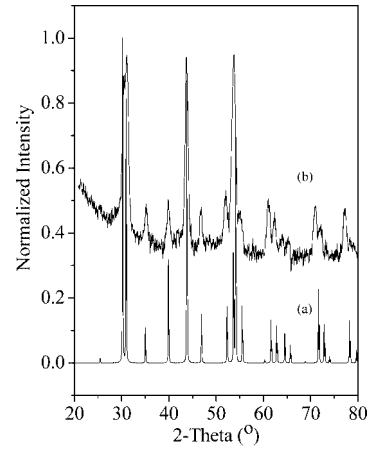

Figure 1. XRPD analysis of (a) calculated reference pattern of $NaGdF_4$ single crystal and (b) $NaGdF_4$ nanoparticles co-doped with 1 mol % Ho^{3+}/20 mol % Yb^{3+}.

The precursors were prepared via addition of a 10 mL mixture of water/trifluoroacetic acid (1:1) to a round-bottom flask containing 2.50×10^{-5} mol of Ho_2O_3 (0.0094 g, 2 mol % Ho^{3+}), 2.50×10^{-4} mol of Yb_2O_3 (0.0985 g, 20 mol % Yb^{3+}), and 9.75×10^{-4} mol of Gd_2O_3 (0.3534 g). The cloudy solution was left to reflux at 80 °C in excess of 12 h until it was clear. The solution was then heated to dryness at 60 °C for several hours to evaporate the water/trifluoroacetic acid. Note that the 1 and 5 mol % Ho^{3+} precursors were prepared in a similar fashion by adjusting the quantities of Ho_2O_3 relative to Gd_2O_3.

In the second step of the synthetic procedure, 12.5 mL of oleic acid and 12.5 mL of 1-octadecene were added to a 3-neck round-bottom flask (solution A). Approximately 2.50×10^{-3} mol of CF_3COONa were added to the dried precursor solids along with 7.5 mL of oleic acid and 7.5 mL of 1-octadecene (solution B). Both solutions were degassed at 150 °C for 30 min under a gentle flow of argon gas to remove any moisture present. Subsequently, solution A was heated to 340 °C and was held at that temperature for several minutes. Addition of solution B to solution A was carried out using a syringe and pump system at a rate of 1.5 mL/min (Harvard Apparatus Econoflow). After 10 min, the system temperature was reduced to 335 °C and was left to stir vigorously for 90 min. The solution was allowed to cool to room temperature. Nanoparticles were precipitated out using absolute ethanol and were isolated via centrifugation (3000 rpm, 15 min). The solids were washed with a 1:8 hexane/ethanol mixture twice to remove any impurities.

Polyacrylic acid (PAA M_{wt} 1800), diethylene glycol (99%), and toluene (>99.5%) were all purchased from Sigma-Aldrich. The ligand exchange procedure was carried out to exchange the oleic acid ligand with poly(acrylic acid) (PAA M_{wt} 1800, Sigma-Aldrich) using an experimental procedure previously described in the work of Zhang et al.[12b] but modified as follows: the diethylene glycol (DEG)/PAA solution was heated under argon to 110 °C. The toluene solution containing 1 wt % nanoparticles was injected in the system at a rate of 2 mL/min and was refluxed afterward for 2.5 h at 150 °C. The cloudiness of the solution decreased on heating. The toluene

(15) Auzel, F. *C. R. Acad. Sci. B, Phys.* **1966**, *262B*, 1016.
(16) Auzel, F. *C. R. Acad. Sci., Ser. B: Sci. Phys.* **1966**, *262B*, 1016.
(17) Buissette, V.; Huignard, A.; Gacoin, T.; Boilot, J. P.; Aschehoug, P.; Viana, B. *Surf. Sci.* **2003**, *532−535*, 444.
(18) Du, Y.-P.; Zhang, Y.-W.; Sun, L.-D.; Yan, C.-H. *J. Phys. Chem. C* **2008**, *112*, 405.
(19) Ghosh, P.; Oliva, J.; De la Rosa, E.; Haldar, K. K.; Solis, D.; Patra, A. *J. Phys. Chem. C* **2008**, *112*, 9650.
(20) Kamimura, M.; Miyamoto, D.; Saito, Y.; Soga, K.; Nagasaki, Y. *Langmuir* **2008**, *24*, 8864.
(21) Sivakumar, S.; Diamente, P. R.; van Veggel, F. C. J. M. *Chem.-Eur. J.* **2006**, *12*, 5878.
(22) Vetrone, F.; Boyer, J.-C.; Capobianco, J. A.; Speghini, A.; Bettinelli, M. *J. Appl. Phys.* **2004**, *96*, 661.
(23) Aebischer, A.; Heer, S.; Biner, D.; Krämer, K.; Haase, M.; Guedel, H. U. *Chem. Phys. Lett.* **2005**, *407*, 124.
(24) Burns, J. H. *Inorg. Chem.* **1965**, *4*, 881.
(25) van der Kolk, E.; Dorenbos, P.; Krämer, K.; Biner, D.; Güdel, H. U. *Phys. Rev. B* **2008**, *77*, 125110/1.
(26) Boyer, J.-C.; Vetrone, F.; Cuccia, L. A.; Capobianco, J. A. *J. Am. Chem. Soc.* **2006**, *128*, 7444.
(27) Zhang, Y.-W.; Sun, X.; Si, R.; You, L.-P.; Yan, C.-H. *J. Am. Chem. Soc.* **2005**, *127*, 3260.

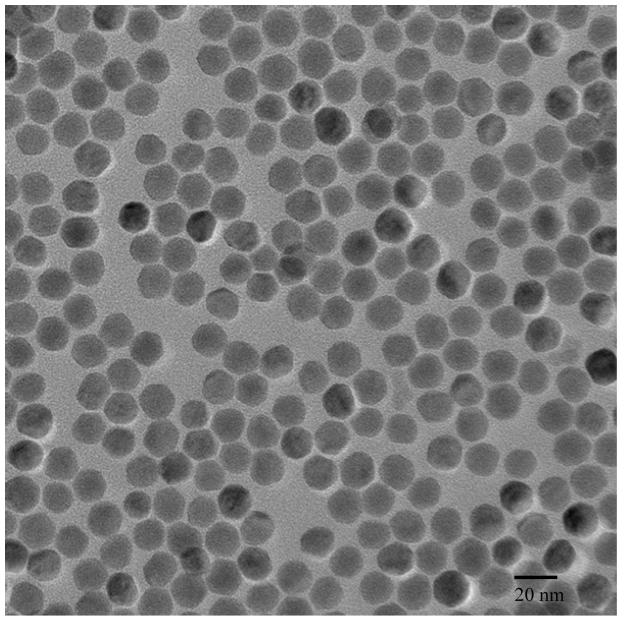

(a)

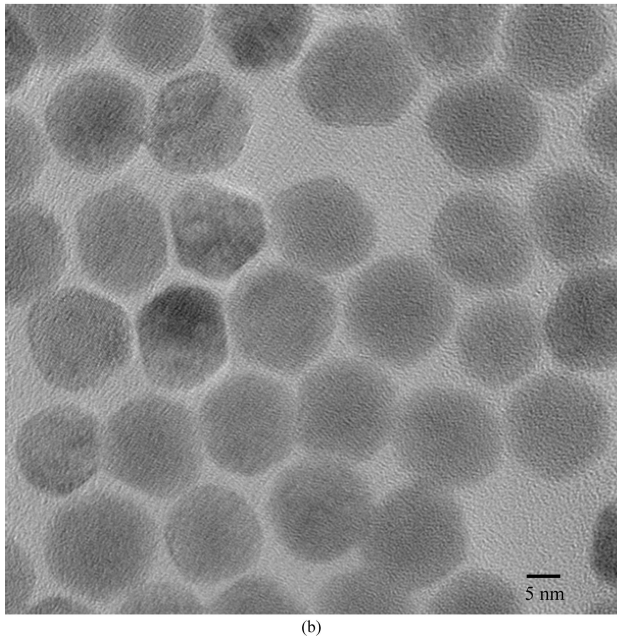

(b)

Figure 2. TEM micrographs of 1 mol % Ho^{3+}/20 mol % Yb^{3+} co-doped $NaGdF_4$ nanoparticles at (a) 100 000× magnification and (b) 300 000× magnification.

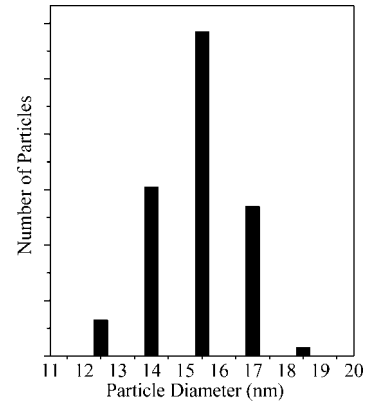

Figure 3. Particle size distribution (PSD) of 1 mol % Ho^{3+}/20 mol % Yb^{3+} co-doped $NaGdF_4$ nanoparticles following TEM analysis.

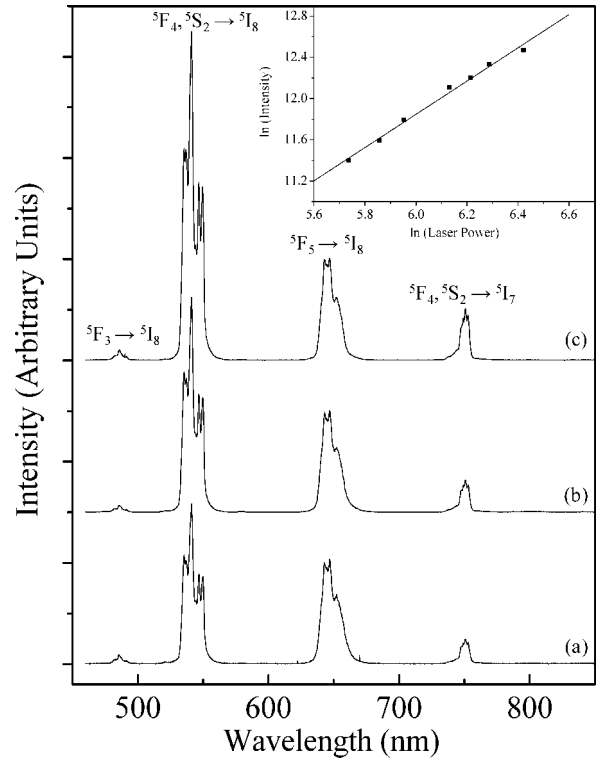

Figure 4. Upconversion emission spectra of $NaGdF_4$ nanoparticles co-doped with Ho^{3+}/Yb^{3+} (a) 1 mol % Ho^{3+}/20 mol % Yb^{3+}, (b) 2 mol % Ho^{3+}/20 mol % Yb^{3+}, (c) 5 mol % Ho^{3+}/20 mol % Yb^{3+}Inset: upconversion power study plot for the $^5F_4, ^5S_2 \rightarrow ^5I_8$ transitions in $NaGdF_4$ nanoparticles co-doped with 1 mol % Ho^{3+}/20 mol % Yb^{3+}.

was then allowed to evaporate by heating the solution (without reflux) to 240 °C for 30 min. The resultant solution was cooled down to room temperature and treated with 0.1 N HCl solution. The precipitated solids were recovered via centrifugation (3000 rpm, 15 min) and washed three times with deionized water. Reionizing the carboxylic groups with 0.1 N NaOH renders them dispersible in water.

Oxidation of the oleic acid ligand was carried out as previously reported in the work of Chen et al.;[13] however, the reaction time was modified from 1 to 48 h to study the extent of ligand oxidation as a function of heating time.

Transmission electron microscopy (TEM) measurements of the colloidal dispersion of nanoparticles were performed with a Philips CM200 microscope operating at 200 kV equipped with a charge-coupled device (CCD) camera (Gaten). Approximately 1 mg of nanoparticles was dispersed in 1 mL of toluene to yield an approximate 0.1 wt % solution. A drop of the resulting solution was evaporated on a Formvar/carbon film supported on a 300 mesh copper grid (3 mm in diameter).

XRPD patterns were measured using a Scintag XDS-2000 diffractometer equipped with a Si(Li) Peltier-cooled solid state detector, Cu Kα source at a generator power of 45 kV and 40 mA, divergent beam (2 mm and 4 mm), and receiving beam slits (0.5 mm and 0.2 mm). Scan range was set from 20−80° 2θ with a step size of 0.02° and a count time of 2 s. The sample was measured using a quartz zero background insert disk.

Visible emission from the $NaGdF_4$:Ho^{3+}/Yb^{3+} nanoparticles was obtained upon excitation with 980 nm using a Coherent 6-pin fiber-coupled F6 series 980 nm laser diode (maximum power of 800 mW at 1260 mA), coupled to a 100 μm (core) fiber. For the spectroscopic studies, the sample was dispersed in toluene (1 wt %) and placed in a Hellma, QS quartz cuvette (1 cm path length).

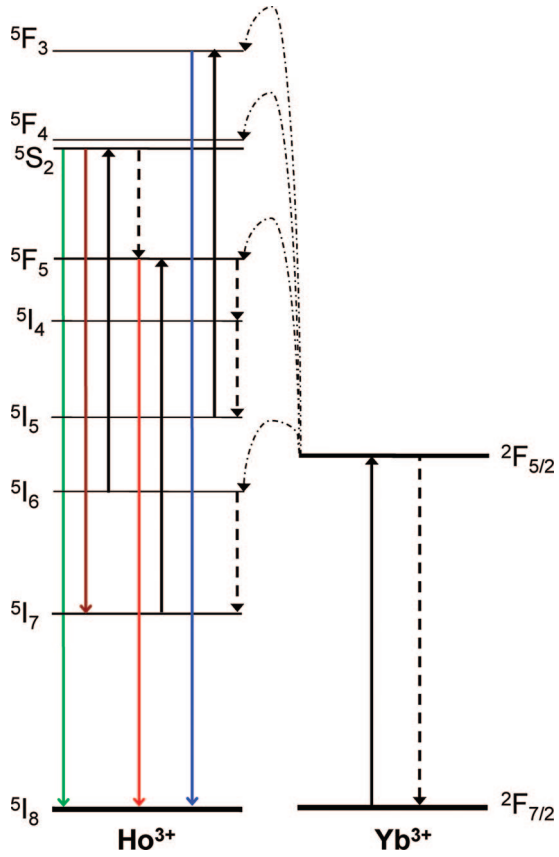

Figure 5. Proposed upconversion mechanism in Ho^{3+}/Yb^{3+} co-doped $NaGdF_4$ nanoparticles using an excitation wavelength of 980 nm. Solid lines indicate excitation, curved arrows indicate energy transfer, and dashed arrows indicate nonradiative decay while colored arrows indicate emission.

The upconverted visible emissions were collected at $\pi/2$ with respect to the incident beam and then dispersed by a 1 m Jarrell-Ash Czerny-Turner double monochromator with an optical resolution of ~0.15 nm. The visible emissions from the sample exiting the monochromator were detected by a thermoelectrically cooled Hamamatsu R943-02 photomultiplier tube. A preamplifier, model SR440 Standard Research Systems, processed the photomultiplied signals, and a gated photon counter model SR400 Standard Research Systems data acquisition system was used as an interface between the computer and the spectroscopic hardware. The signal was recorded under computer control using the Standard Research Systems SR465 software data acquisition/analyzer system.

Results and Discussion

X-ray powder Diffraction Analysis of $NaGdF_4$:Ho^{3+}/Yb^{3+} Nanoparticles. X-ray powder diffraction analysis was used to characterize the $NaGdF_4$ nanoparticles. Sodium gadolinium fluoride can exist in two phases, namely, cubic (α-phase) and hexagonal (β-phase). The XRPD diffraction pattern is shown in Figure 1 with the results suggesting that the nanoparticles are in fact hexagonal since the observed pattern is similar to that of reference hexagonal $NaGdF_4$ reported in JCPDS 27-699, as well as the reference pattern of the hexagonal $NaGdF_4$ single crystal.[28] Similar results were observed for the 2 and 5 mol % Ho^{3+}/20 mol % Yb^{3+} nanoparticles. The luminescence of the hexagonal nanoparticles is known to be at least 1 order of magnitude greater than that of their cubic counterpart.[23] Following oleic acid ligand modification and/or ligand exchange coupled by dispersion in water (discussed later), it is expected that the luminescence of the nanoparticles would decrease principally due to the presence of water. The presence of OH groups with phonon energies of ~3500 cm^{-1} would inevitably lead to an increase in nonradiative pathways. The probability of bridging the energy gaps therefore increases significantly. It follows that the desired phase for the synthesized nanoparticles is the hexagonal phase due to the increased luminescence in comparison to the cubic phase.

Transmission Electron Microscopy (TEM) Analysis of $NaGdF_4$:Ho^{3+}/Yb^{3+} Nanoparticles. TEM was used to evaluate the morphology and particle size distribution (PSD) of the prepared nanoparticles. The TEM micrographs are shown in Figure 2. The thermal decomposition synthesis described above resulted in hexagonal-shaped nanocrystals with an extremely narrow PSD. Approximately 500 particles were evaluated to obtain the distribution summarized in Figure 3. Statistical analysis showed a mean particle size of 15.6 ± 1.2 nm, with a range between 13−19 nm. The strict particle size control occurs as a result of the mechanical pump addition of the precursor solution that ensures a constant rate of addition to the ligand pot heated at 310 °C. Consequentially, the trifluoroacetate precursors experience a similar environment upon decomposition at temperatures in excess of 280 °C. Uneven addition of the precursor solution, typically heated at 135 °C, could otherwise result in sudden temperature fluctuations causing improper and incomplete particle formation and growth. It follows that subsequent modifications to the nanoparticles through ligand exchange or ligand cracking occur in a more uniform and even fashion.

Upconversion Luminescence of $NaGdF_4$:Ho^{3+}/Yb^{3+} following 980 nm Excitation. Following 980 nm excitation, visible upconversion emission was observed for all the $NaGdF_4$:Ho^{3+}/Yb^{3+} nanoparticles under investigation (Figure 4). Blue as well as predominantly green upconversion luminescence was observed for transitions centered at 486 nm and 541 nm and corresponding to the emission from the $^5F_3$ and $^5F_4$, $^5S_2$ levels to the $^5I_8$ ground state, respectively. The notably weaker red and NIR upconversion luminescence (relative to the green emission) was observed at 647 and 751 nm and was ascribed to the transition from the $^5F_5 \rightarrow {}^5I_8$ and $^5F_4$, $^5S_2 \rightarrow {}^5I_7$ states, respectively. The upconversion spectra in Figure 4 were normalized to the red emission observed at 647 nm and reveal an increase in the green emission as a function of increasing Ho^{3+} ion concentration in the co-doped system. For the 1 mol % Ho^{3+}/20% mol % Yb^{3+}, a green:red intensity ratio of 1.47 was observed and increases gradually to 1.53 and 1.57 as the Ho^{3+} concentration is raised to 2 and 5 mol % in the co-doped nanoparticles. It should be noted that the NIR emission emanating from the $^5F_4$, $^5S_2 \rightarrow {}^5I_7$ levels also increases as a function of the Ho^{3+} concentration since this peak originates from the same excited states ($^5F_4$, $^5S_2$) as the green transition. The overall upconversion emission intensity increases as the Ho^{3+}concentration increases since more ions become available to undergo the energy transfer process with the Yb^{3+} ions. The increase in efficiency of the energy transfer process hence will contribute to a more intense luminescence.

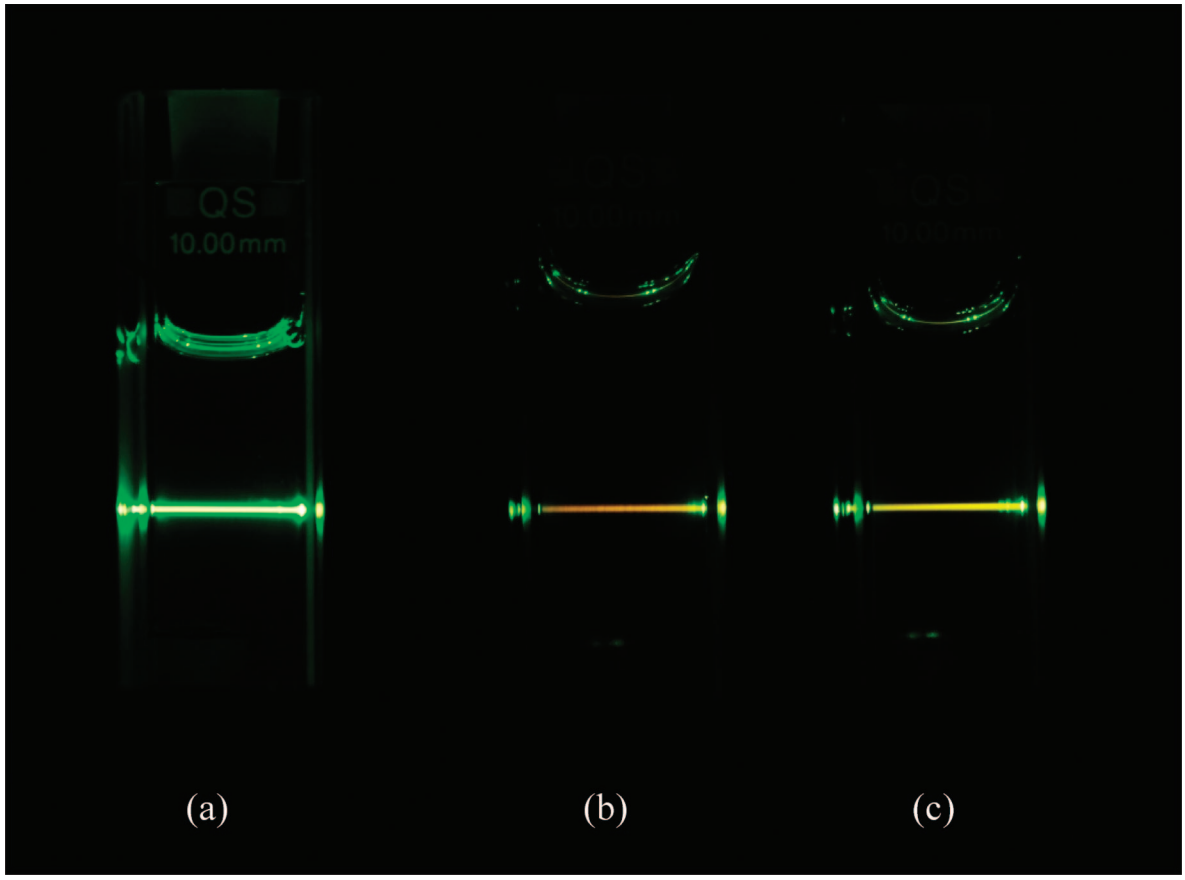

Figure 6. Visual observation of upconversion emission using an excitation wavelength of 980 nm for Ho^{3+}/Yb^{3+} co-doped $NaGdF_4$ nanoparticles (a) dispersed in toluene, (b) dispersed in water following oxidation of the oleic acid ligand, and (c) dispersed in water following exchange of the oleic acid ligand with PAA.

Upconversion Luminescence Power Study of $NaGdF_4$: Ho^{3+}/Yb^{3+} following 980 nm Excitation. An upconversion power dependence study was carried out to determine the number of photons involved in the upconversion mechanism (see inset in Figure 4). In this study, the natural log of the pump power was plotted versus the natural log of the upconversion emission intensity.[29] A linear regression fit was used, and a slope value of 2.04 was obtained for the upconverted green emission from the $^5F_4$, $^5S_2 \rightarrow {}^5I_8$ states of Ho^{3+} indicating a two-photon mechanism was operative. The upconversion mechanism is shown in Figure 5. The tripositive holmium ion does not have an energy level resonant with 980 nm, which corresponds to the excitation wavelength of the diode; this suggests that the upconversion process is initiated by first raising the Yb^{3+}ion to the $^2F_{5/2}$ excited-state via an incoming pump photon.[30] The subsequent step involves an energy transfer to the Ho^{3+} $^5I_6$ or $^5I_7$ intermediate excited states. Once the two states are populated, an incoming pump photon or a second ET from a neighboring Yb^{3+} ion may result in the population of the $^5F_4$, $^5S_2$, and $^5F_5$ Ho^{3+} states, respectively. Population of the $^5F_5$ state may also occur via a nonradiative decay from the higher lying $^5F_4$, $^5S_2$ levels; however, this mechanism requires several phonons to bridge the gap separating the energy levels and does not contribute significantly to the enhancement of the $^5F_5$ red emission. This can be seen from Figure 4 where the green emission is observed to increase as the Ho^{3+} concentration increases (as previously discussed). Blue upconversion emission occurs through the initial population of the $^5I_5$ level via nonradiative decay from the upper lying $^5F_5$ and $^5I_4$ states. This is subsequently followed by an ET from the $^2F_{5/2}$ excited-state of Yb^{3+} raising the ion to the $^5F_3$ excited-state and blue emission ensues.

Modification of the Hydrophobic Oleic Acid Ligand for Water Dispersibility: Oxidation of the Oleic Acid. To render the nanoparticles more amenable to dispersion in water, a modification of the oleic acid ligand is required be it via alteration of the ligand itself or complete substitution with a more water miscible ligand. One approach undertaken consisted of the use of a strong oxidizing agent (permanganate/periodate) to break the double bond of the long C18 chain.[13,31] Hence, the double bond of the $C_9{=}C_{10}$ carbons is exploited. The chain is shortened by nine $-CH_2-$ units and terminated with a carboxylic acid group. Thus, the permanganate oxidation of the oleic acid yields azelaic acid. The $-$COOH moiety, which has H-bonding capabilities, is maintained, and the alkane chain is shortened (alkene bond is lost), which can allow for better dispersibility in water or

(28) Brunton, G. D.; Insley, H.; McVay, T. N.; Thoma, R. E. ORNL-3761; United States Atomic Energy Commission: 1965.
(29) Chamarro, M. A.; Cases, R. *J. Lumin.* **1990**, *46*, 59.
(30) Johnson, L. F.; Guggenheim, H. J.; Rich, T. C.; Ostermayer, F. W. *J. Appl. Phys.* **1972**, *43*, 1125.
(31) Lemieux, R. U.; von Rudloff, E. *Can. J. Chem.* **1955**, *33*, 1701.

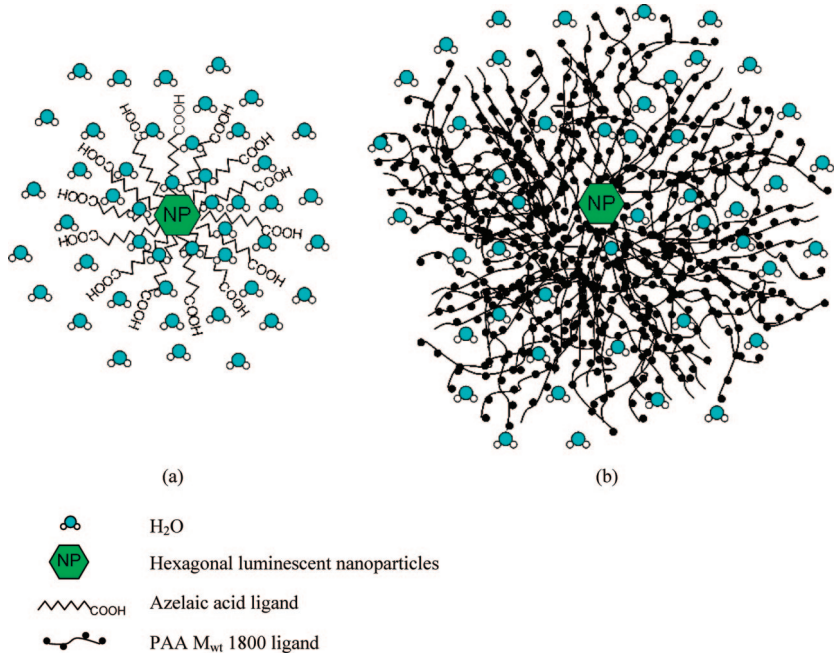

Figure 7. Exposure of the luminescent core of Ho^{3+}/Yb^{3+} co-doped $NaGdF_4$ nanoparticles to water following (a) oxidation of the oleic acid capping ligand and (b) ligand exchange with PAA M_{wt} 1800.

other aqueous solvents. In this reaction, the hydrophobicity of the molecule is decreased while the hydrophilicity is increased.

The oxidized nanoparticles were evaluated after 1, 2, 4, 24, and 48 h. No significant improvement in luminescence was observed beyond the 2 h reaction time suggesting that the oxidation reaction has practically achieved completion by that time. Prolonged oxidation resulted in the formation of a brown MnO_2 precipitate which could not be easily separated from the upconverting nanoparticles. As a result, the particles were less amenable to dispersion in water and showed weak upconversion luminescence intensity.

It is noteworthy to mention that the upconversion emission decreases on modification of the oleic acid and changing the dispersion medium from toluene to water. The shorter chain length of the C9 azelaic acid does not shield the luminescent nanoparticles as efficiently as the longer C18 oleic acid ligand. The water molecules are also capable of contributing high phonon energies, which favor the nonradiative relaxation pathways for the Ho^{3+} and Yb^{3+} ions. A comparison of the visible emission, observed visually, of the oxidized and parent nanoparticles prepared at 1 wt % solutions is shown in Figure 6. Aqueous solutions of the oxidized nanoparticles prepared using a reaction time of 1−4 h were stable for up to 1 week in water after which precipitation of the nanoparticles was observed.

Modification of the Hydrophobic Oleic Acid Ligand for Water Dispersibility: Ligand Exchange of the Oleic Acid. A second and perhaps a more versatile approach involves the complete exchange of the oleic acid molecule with a hydrophilic ligand. In the case of the oxidation of the double bond of oleic acid, a terminal −COOH group is the ultimate result. Further chemistry would be required to substitute the carboxylic acid terminal with $-NH_2$, SO^{3-}, and so forth. In the ligand exchange procedure, the selected ligand already possesses the desired terminal ends. As a result, ligand exchange can offer a more interesting alternative to other modification approaches.

The ligand exchange procedure was carried out using poly(acrylic acid) (PAA). Following the exchange with oleic acid, the resultant nanoparticles produced a clear and transparent solution in water (prepared at 1 wt %). Furthermore, the resultant nanoparticles showed moderate upconversion emission, which was slightly brighter relative to the oxidized particles (Figure 6). The PAA ligand may be more effective at shielding the luminescent core from the water relative to the oxidized C9 chain. It is noteworthy to mention that the parent nanoparticles, dispersed in toluene, resulted in green upconversion emission, while the modified nanoparticles dispersed in water resulted in a more yellow upconversion emission likely due to the increase in the red component. The probability of the latter increases as the nonradiative decay pathways become prominent in water due to the higher phonon energy availability. The oxidized nanoparticles showed a higher red component in the upconversion luminescence. This is expected as the C9 molecules of azelaic are not as effective in protecting the luminescent core in comparison to the long PAA chains (see Figure 7).

The physical stability of the modified ligand was evaluated in water and phosphate buffer saline, pH 7.4 (PBS). The modified nanoparticles showed prolonged stability for greater than 3 months when dispersed in water with no noticeable decrease in luminescence. In contrast, stability in PBS was less than 24 h and may be due to the high ionic strength of the aqueous medium.

Conclusions

A thermal decomposition synthetic route was used to prepare highly monodisperse upconverting $NaGdF_4$ co-doped with 1−5 mol % Ho^{3+}/20 mol % Yb^{3+}. The uniform addition of the precursor solution resulted in a very narrow PSD of

approximately 15 nm. The oleic acid-capped hexagonal nanoparticles showed strong upconversion luminescence once dispersed in an organic nonpolar medium. Two strategies to render the hydrophobic nanoparticles dispersible in water were evaluated and gave similar results. A complete ligand exchange with PAA resulted in moderate upconversion luminescence intensity as well as physical stability of the dispersed nanoparticles in solution for up to 3 months. Studies targeting functionalization of the water dispersible nanoparticles for biological applications have been initiated and will be the subject of a future publication.

Acknowledgment. The authors wish to thank the Natural Sciences and Engineering Research Council (NSERC) of Canada and the Gouvernement du Québec, Ministère du Développement économique, de l'Innovation et de l'Exportation for funding.

Note Added after ASAP Publication. Reference 12b was missing in the version published ASAP January 22, 2009; the corrected version was published February 17, 2009.

CM803151Y